

# Adaptive Optics for High-Contrast Imaging

Markus Kasper\*<sup>a</sup>

<sup>a</sup>ESO, Karl-Schwarzschild-Str. 2, 85748 Garching, Germany;

## ABSTRACT

The paper motivates the science requirements for high-contrast imaging illustrated by actual observation results. After an introduction to the high-contrast-imaging problem composed of extreme adaptive optics, coronagraphy, wave-front control and post-processing, the state-of-the-art will be reviewed putting emphasis on existing instruments and those that are near completion: LBT-FLAO, Magellan Mag AO, Palomar P3K / P1640, Subaru SCExAO, Gemini GPI, and VLT SPHERE.

**Keywords:** Extreme Adaptive Optics, High-contrast Imaging, Exoplanets

## 1. INTRODUCTION

The existence of Exoplanets in large numbers has been predicted since a long time. Epicurus (300 BC) stated “There are infinite worlds both like and unlike this world of ours inhabited by living creatures and plants and other things we see in this world”, and Giordano Bruno (1584) added “There are countless suns and countless earths all rotating around their suns in exactly the same way as the seven planets of our system ...these worlds are no worse and no less inhabited than our Earth”. While infinite and countless numbers of terrestrial Exoplanets yet remain to be confirmed, the evidence constituted by almost 800 confirmed detections of Exoplanets (July 2012, [exoplanet.eu](http://exoplanet.eu)) and more than 2000 further candidates ([kepler.nasa.gov](http://kepler.nasa.gov)) as well as indications that in average every star is orbited by at one or more rocky planets [1,2] points in this direction.

### 1.1 Direct imaging motivation

Only a very small number of the presently known Exoplanets were discovered by direct imaging, i.e. by spatially separating the photons from the Exoplanet from the ones emitted by its host star. The main reasons for this deficiency are the enormous technological challenges that have to be overcome in order to reach the required subarcsecond separation contrast levels of  $10^{-5}$  for self-luminous giant planets down to  $10^{-10}$  for an Exoearth orbiting a G-star in its habitable zone. The most successful Exoplanet observing techniques today exploit i) radial velocity (RV) changes of the star orbiting around the center of gravity of the star-planet system or ii) photometric changes of the star when obscured by a transiting exoplanet orbiting in front of it as seen from Earth. The transit method even offers the possibility to obtain spectral information from the Exoplanet via secondary transits or transmission spectroscopy. While secondary transits overcome the brightness ratio between star and planet by observing close-in planets preferably in the MIR, transmission spectroscopy is independent from the orbital separation between star and planet but depends on the extent of the optically thin atmosphere. For the case of an Exoearth, the required photometric precision would be of the order  $10^{-6}$ - $10^{-7}$  for the most prominent spectral features [5], and the interpretation of the data is complicated by the unknown stratification of the atmosphere.

Direct imaging offers unique observation capabilities. It is presently the most promising technique to efficiently reduce photon noise generated by the host star by suppressing its light intensity while maintaining the one of the Exoplanet. At a spectral resolution of  $\sim 30$ , a 5<sup>th</sup> magnitude star provides about  $10^{12}$  photons per hour in an 8-m telescope aperture. This would be just enough for a one sigma detection of a  $10^{-6}$  signal, and 25 hours of observation are needed for the commonly accepted 5 sigma detection. For lower contrasts, i.e. all but the shortest period planets seen in reflected light and heated by the stellar radiation, the detection of Exoplanetary photons requires suppression of stellar light. Planet-formation is another science case where direct imaging is most efficient. Giant planets are expected to form close to the

ice-line at a few AU, which is an orbital separation hardly accessible for RV and transit methods whose detection capabilities are biased towards small orbits.

In addition, direct imaging offers important complementary information such as resolving the  $\sin i$  ambiguity intrinsic to the RV method and allow for dynamic mass measurements of individual Exoplanets. It provides additional diagnostic data, e.g., through polarimetry, and greatly improves observing efficiency through confirming a detection in a couple of nights rather than following an orbit.

## 1.2 Present results

When astronomers started to realize that the detection of young self-luminous giant planets by ground-based direct imaging is feasible a large number of surveys were initiated by different groups (e.g. [6-13]). In total, these surveys targeted a couple of hundred young stars of spectral types B-M, typically located within 80 pc. They used ground-based AO-assisted NIR or L-band imaging with or without coronagraphy and typically achieved NIR contrasts of  $10^{-4} - 10^{-5}$  at  $0.5'' - 1''$  separation.

None of these surveys detected any Exoplanets, and the science was limited to determining detection limits and analyzing the constraints on models describing the expected abundance of Exoplanets as a function of orbital separation as depicted in Figure 1. The main conclusion from these surveys is that young giant Exoplanets are exceedingly rare at orbital separations larger than about 20 AU

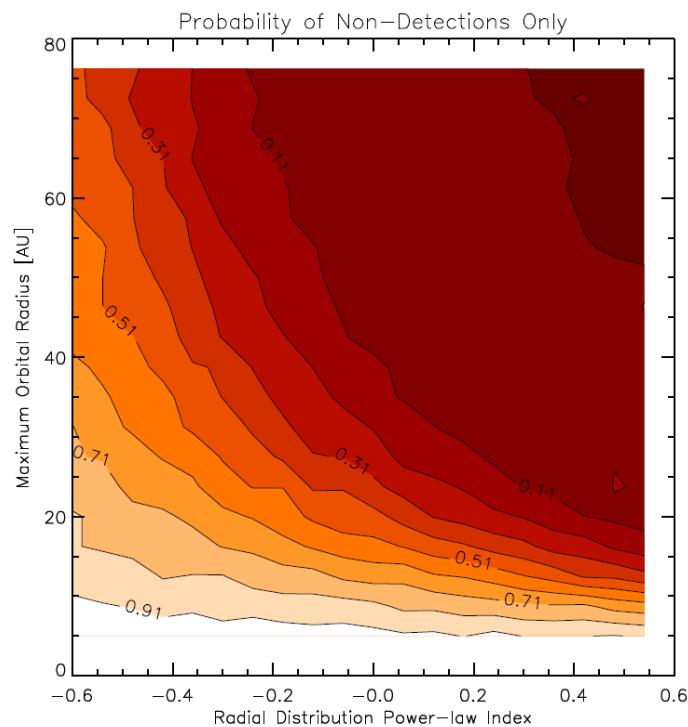


**Figure 1.** Map of probability that the planet population simulated for a given radial power-law index and a maximum cut-off radius is consistent with the only non-detections in the survey (from [9]).

Fortunately the challenges imposed by high-contrast imaging have encouraged researchers and engineers to put a lot of effort into the development of numerous techniques that are introduced in the next section. These efforts are now starting to pay off as the first Exoplanets have recently been imaged around the young A-stars with debris disks HR 8799 [3] and beta Pictoris [4]. Almost fifty refereed papers (33 on HR8799 and 15 on beta Pictoris) were published based on observations of these two stars over the past three years since the detection of the their planets. The science objectives

cover a wide range from measuring the orbits, and aligning them with the debris disks, over comparing the spectra to theoretical model predictions to testing novel observing techniques.

### 1.3 Contrast requirements

The main reason for which the number of direct imaging detections of Exoplanets is still small is shown in Figure 2 presented in [14]. While currently achievable contrasts ( $\sim 10^{-5}$  at 0.5" separation) just scratch on the population of self-luminous warm, the upcoming high-contrast imaging instruments introduced hereafter with expected imaging contrasts of typically  $10^{-6}$  at 0.2" and  $10^{-7}$  at 0.5" are well suited for the detection of a larger number of such Exoplanets. In order to reach down to Jupiters, Neptunes and eventually rocky planets observed in reflected light, one must push towards higher contrasts or smaller inner working angles. Ground-based observations fundamentally suffer from photon noise created by residual aberrations of the AO corrected atmospheric turbulence and can hardly go beyond  $10^{-9}$  contrast in reasonable observing times of a few hours even for the next generation of extremely large telescopes. Due to the large telescope diameter of the order 30-40 m, they can however push the inner working angle to 10-20 mas in the NIR gaining access to even rocky planets around nearby stars [15]. Space-based telescopes instead have limited angular resolution because aperture sizes are limited by economical and technological reasons, but can go down to  $10^{-10}$  contrast at about 0.1" using advanced coronagraphy and wave-front control.

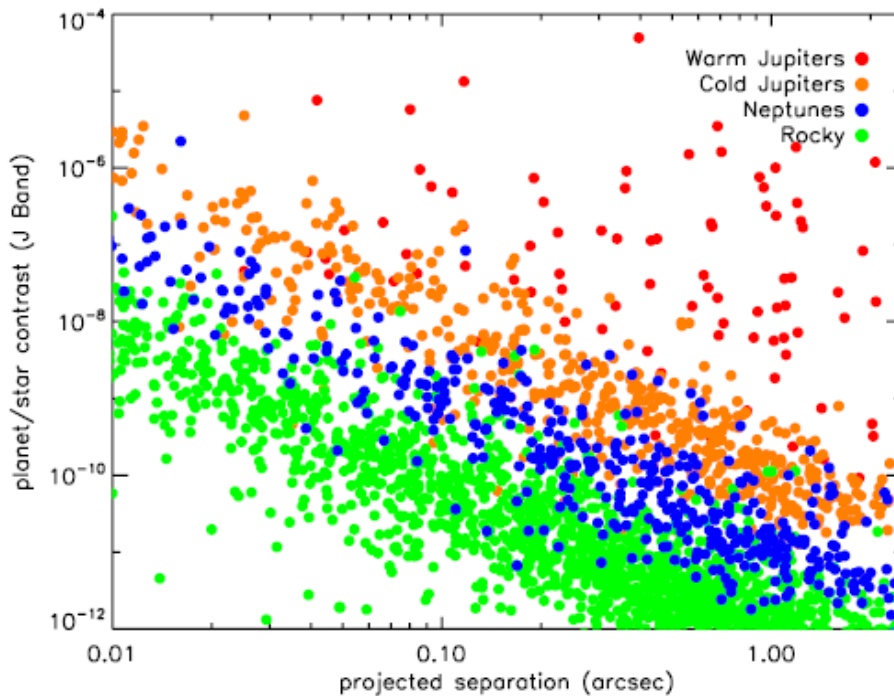


**Figure 2.** Planet/star contrast vs. projected separation for a sample of sample of 600 nearby ( $d < 20$  pc) stars selected from the Hipparcos catalogue assuming 5 planets per star with an empirically determined orbital distribution (from [14])

## 2. HIGH-CONTRAST IMAGING PILLARS

Highest contrast observations from the ground require multiple correction stages to correct for i) atmospheric turbulence, ii) aperture diffraction, and iii) quasi-static instrumental aberrations. As depicted in Figure 3, a so-called eXtreme Adaptive Optics (XAO) system corrects the dynamic aberrations introduced by the turbulent atmosphere to very high levels significantly better than 100nm rms residual wave-front error corresponding to some 90% Strehl ratio in the NIR. Still, the Airy pattern of the telescope aperture shows a ring-like (for nearly circular apertures) structure modulated and sprinkled by quasi-static speckles from instrumental aberrations with intensity that is up to  $10^{-3}$  of the peak intensity at small angular separations. However, it is in principal possible to almost completely remove the Airy pattern even at

smallest angular separation by means of coronagraphy and correct for the quasi-static speckles using the deformable mirror of the XAO system. Finally, speckles and real faint companions have different polarimetric, spectral, coherence and field-dependent properties that can be used to tell them apart and be able to detect companions at levels of one part in a billion of the stellar light. This is sufficient to observe Exoplanets in reflected light around nearby stars at small angular separations (see Figure 2).

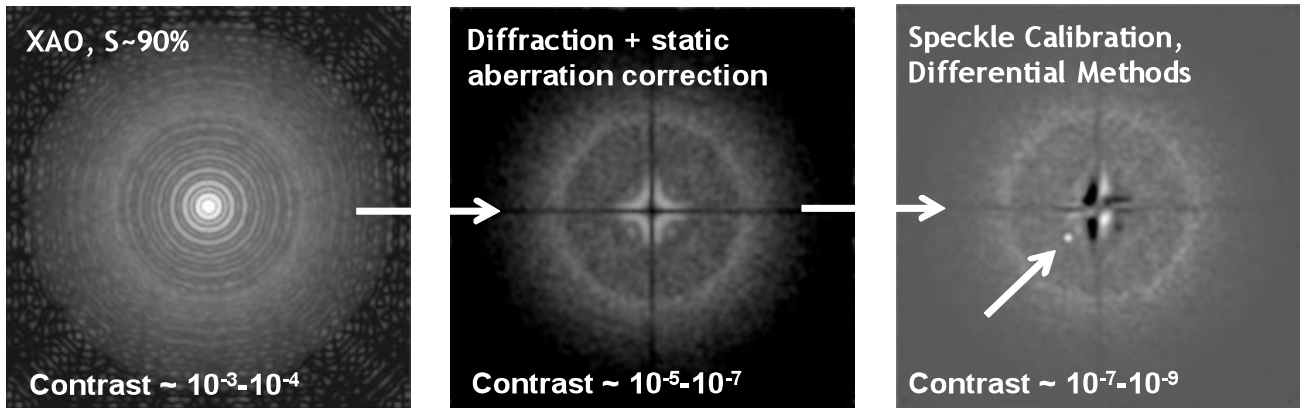


**Figure 3.** Generic ground-based high-contrast imaging recipe.

## 2.1 Extreme Adaptive Optics (XAO)

The Center for Adaptive Optics defines on its webpage (<http://cfao.ucolick.org/>) that XAO is "...scientifically driven by the need to achieve high-contrast imaging and spectroscopic capabilities to enhance the detection and characterization of extra-solar planetary systems...". This definition is scientifically motivated and directly links XAO to high-contrast imaging and Exoplanet science making it a special case. All other flavors of Adaptive Optics such as ground-layer AO (GLAO), laser-tomography AO (LTAO), multi-conjugate AO (MCAO) etc. are motivated by technology and describe a particular setup of wave-front sensors, DMs and control algorithm.

Typically, XAO systems are designed as standard Single Conjugate AO systems with many degrees of freedom and high temporal correction bandwidth. As two of the dominant terms in the error budget (fitting error and temporal bandwidth error) are strongly reduced this way, such an AO system provides a high Strehl ratio in the NIR maximizing the intensity in the PSF core and hence the Exoplanet signal. The correction quality is usually still good enough for diffraction limited images in the optical part of the spectrum. However, the stellar halo intensity is proportional to the spatial power spectrum of the residual wavefront aberrations (e.g. [16]), and the DM can suppress these aberrations up to its correction radius  $\theta_{AO} = \lambda/(2d)$ , where  $\lambda$  is the wavelength of the observation and  $d$  is the interactuato spacing projected back to the telescope aperture.

Since Exoplanets are most easily found at small angular separations (see Figure 2), a very efficient and precise correction of low spatial frequency aberrations, i.e., low-order modes, to achieve a high-contrast ("dark hole") close to the PSF center is a prime objective of an XAO system. Unfortunately, it is at low spatial frequencies where the commonly used Shack-Hartmann sensor (SHWFS) has the lowest sensitivity. The non-modulated or fixed Pyramid wave-front sensor (FPYRWFS) instead provides excellent low spatial frequency performance [16] and still a high elevated technological readiness level since it has already been tested in the lab and on-sky [17,18]. There, the sensitivity gain of the FPYRWFS over the SHWFS is of the order  $D/r_0$  [16,19], where  $D$  is the telescope aperture diameter and  $r_0$  is the Fried-parameter.

Figure 4 shows the error budget of an XAO system for an extremely large telescope. In this case the simulated system used a FPYRWFS running at 3 kHz framerate. It can be seen that the in-band wave-front error, i.e., the residual aberrations in the spatial frequency range that can be corrected by the DM, is dominated by two terms: i) the refractive index chromaticity ("chromatic index") and ii) the temporal bandwidth error ("servolag"). Photon noise will soon become the dominant term for stars fainter than the assumed 6th magnitude, aliasing is mostly relevant close to the maximum spatial frequency sampled by the WFS, and chromatic anisoplanatism (light at different wavelengths is seen at different angles because of atmospheric dispersion and hence sample slightly different atmospheric turbulence) is only a minor contributor to the error budget at moderate zenith distances going to zero at zenith.

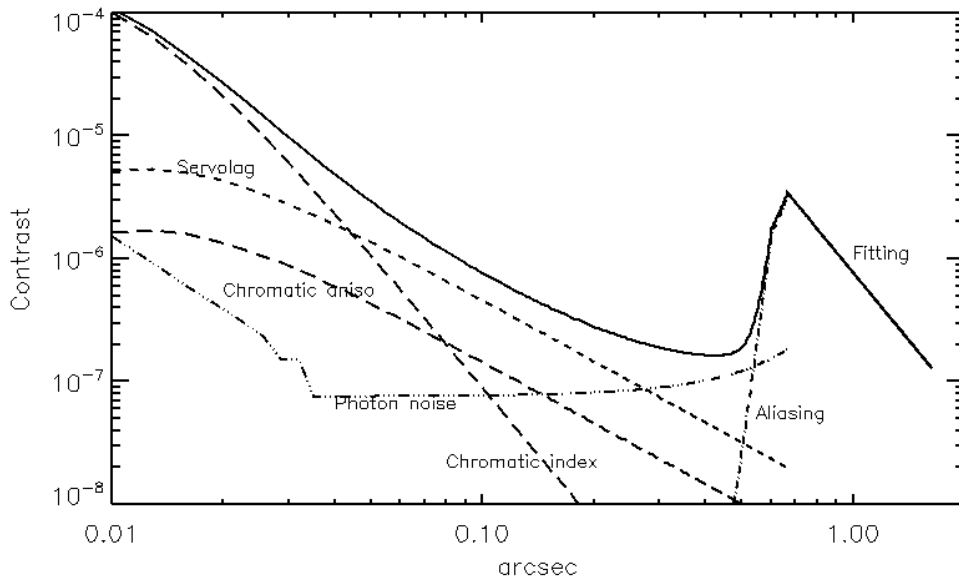


**Figure 4.** AO residual halo contrast.  $I=6$ ,  $0.85''$  seeing, 30 deg zenith distance,  $\lambda = 1.3 \mu\text{m}$

The temporal bandwidth error can be reduced by a higher correction bandwidth, and there are a number of ways in which this can be achieved, e.g. an even faster AO system with higher frame-rates and/or smaller delays, predictive control schemes [20] or other methods that improve the rejection of low frequency aberrations by the control system, e.g. through double integrator control or linear-quadratic-Gaussian (LQG) control.

The refractive index chromaticity derives from the fact that the refractive index of air is a decreasing function of wavelength. If wave-front sensing is done in the visible regime, the near-infrared wave-front is over-compensated by a certain fraction of the visible wave-front [21]. This error term is therefore proportional to the uncompensated wave-front error and relevant only for extremely large telescope. It can be mitigated by choosing the WFS wavelength as close as possible to the science wavelength, and it could even be corrected because the error can be calculated (uncompensated wave-front and refractive index chromaticity of air are known) and off-loaded to the AO system.

The importance of efficient correction of low spatial frequency wave-front errors because of the restrictive inner working angle set by Exoplanet science was emphasized above. In addition, very precise source positioning and tip-tilt correction is also of paramount importance for the small inner working angle coronagraphs which can tolerate displacements of no more than  $1/10 \lambda/D$  [22]. Various concepts were developed to precisely place a spot on the mask [e.g. 23] and efficient tip-tilt correction by the AO system even in the presence of vibrations can be achieved by LQG control [24].

## 2.2 Coronagraphy and wave-front control

A large number of coronagraphs have been developed during the past decades [22], and very recent refinements of the promising vector-vortex coronagraph [25] and phase-induced amplitude apodization coronagraphs [26] are getting very near to the theoretical optimum. As mentioned above, small inner working angle coronagraphs are very sensitive to pointing errors. In addition, it is technologically challenging to achieve very high contrast performance over a finite spectral band (the masks would typically have to have a diameter whose size is a function of wavelength), and they consist of rather complex optical setups involving several phase and/or amplitude masks in pupil and image planes as well as the re-imaging optics.

This added complexity can be avoided by using aperture plane apodization techniques such as apodizing phase plates [APP, 29] or shaped pupils [30], which create PSFs with very deeply suppressed diffraction over certain areas. The conceptual simplicity and robustness of these methods however comes at the expense of a limited field-of-view impacted

observing efficiency and increased liability to stray-light and ghosts since the total intensity of the stellar light passes through the system without being suppressed.

However, no matter how could the coronagraph, instrumental phase and amplitude aberrations will create quasi-static speckles that severely limit the achievable contrast (already 1 nm rms of a sine phase aberration produces a pair of speckles at an intensity contrast of  $5 \times 10^{-6}$  speckle in H-band) if left uncompensated. Fortunately, deep suppression of speckles over a limited part of the PSF is possible through phase correction by the DM. In order to suppress a speckle created by phase and/or amplitude aberrations inside its correction radius, the DM just needs to create an anti-speckle of the same amplitude but with a  $\pi$  phase-shift at the same location. Obviously this scheme would work perfectly for pure phase aberrations in the aperture since the DM would simply have to compensate for the phase aberration. Unfortunately, speckles created by a sine phase aberration with phase  $\theta$ , e.g. created by the DM, have phases  $\pi/2 - \theta$  and  $\pi/2 + \theta$ , while the speckles created by a similar amplitude aberration have phases  $\theta$  and  $-\theta$  [16]. Hence, only one of the amplitude speckles can be suppressed by an aperture plane DM at the expense of an amplification of the other one. Exploiting the Talbot effect, i.e. the transformation of a phase sinusoid into an amplitude sinusoid by Fresnel propagation, it is however possible to correct all image plane speckles over a certain wavelength range using a second DM. Algorithms that describe in more detail how to suppress speckles and create a dark hole with a single DM were presented [e.g. 27]; and a suppression of the diffracted and scattered light near a star-like source to a level of  $6 \times 10^{-10}$  at  $4 \lambda/D$  using such methods has been demonstrated in the laboratory [28].

### 2.3 Differential methods and post-processing

Instrumental aberrations will change with time (atmospheric dispersion will cause the light beam to wander across the instrument optics before the atmospheric dispersion compensator, changing gravity or temperature may introduce flexures of optics, etc.), and they will change with wavelength (refractive optics are not entirely achromatic, the phase and amplitude parts of out-of-pupil instrumental aberrations are modulated depending on wavelength when propagated back to the pupil, etc.). Hence, efficient post-processing of high-contrast imaging data is needed to further improve the contrast. Answers to questions like "how do speckles look like? What are typical intensities and locations? On which time-scales do speckles change? How do speckles change with wavelength? ..." are crucial for defining strategies to overcome the contrast limits set by residual speckles and to ultimately reach the levels required for the detection of Exoplanets.

Chromatic methods include simultaneous differential imaging (SDI) and spectral deconvolution (SD). SDI [32] makes use of the different spectral energy distributions of the star and its companion. One can then define two narrow bands close to each other in wavelength so that in a difference image, the speckles will subtract out but the companion does not (e.g. because methane absorption longwards of  $1.62 \mu\text{m}$  in the cool atmosphere of a late type brown dwarf makes it almost disappear in an image taken at this wavelength). SD [33] makes use of the fact that the radial location of the speckles from the centre of the PSF is proportional to wavelength, while the location of a companion with respect to the star is fixed. SD relies on a reliable method to fit the speckle's spectrum by a model that is largely insensitive to the signal produced by the Exoplanet. It further requires that a certain speckle moves by at least one resolution element between the shortest and the longest wavelength, so small inner working angle can only be obtained when observing over a large spectral range.

Polarimetric differential imaging (PDI) is based on the fact that speckles remain unpolarised while stellar light reflected off an Exoplanet will be polarized to some degree. Thus, if two images at orthogonal polarisations are taken simultaneously and subtracted, the speckles will disappear but the polarized flux from the Exoplanet will remain.

Temporal or statistical methods exploit rapid variations in the speckle pattern. Spurious Speckle intensity is modified by the static complex amplitude (e.g. diffraction pattern) because of interference between the two. This is not the case for the incoherent light from an Exoplanet, so the temporal statistics of intensity fluctuations can be used to differentiate between speckles and real companions [34]

Spatial methods such as angular differential imaging [ADI, 35] can be used if the field of view, and hence the image of the Exoplanet, is allowed to rotate with respect to the telescope/instrument configuration and hence the quasi-static speckle pattern. With suitable processing of such a sequence of images [e.g. 36], one can remove the speckles while enhancing the signal from a companion. ADI is rather simple to implement on alt-azimuth telescopes (field and pupil rotate with respect to each other) and now widely used for high-contrast imaging. ADI requires sufficient field rotation

during the observation to rotate a speckle by at least one resolution element. Depending on the radial distance of the speckle and the object's location on sky, this can translate into rather long observing times for which temporal decorrelation of the quasi-static speckles may occur limiting the efficiency of the method.

Table 1 lists the various post-processing methods and demonstrated performance on-sky. All the methods are good for a reduction of residual speckles and hence an improvement of the final contrast performance by at least a factor 10. Since independent physical properties of light are exploited for each of the methods, it is reasonable to assume that contrast can be improved further by combining several of these methods in series.

**Table 1.** High-contrast imaging post-processing methods.

|  | <b>IWA</b>               | <b>Demonstrated rejection on-sky</b> |
|--|--------------------------|--------------------------------------|
| <b>Spectral Deconvolution</b>                  | $\sim R \cdot \lambda/D$ | $\sim 20$ [31]                       |
| <b>Spectral Differential Imaging (SDI)</b>     | $1 \lambda/D$            | $\sim 10$ [37]                       |
| <b>Angular Differential Imaging (ADI)</b>      | A few $\lambda/D$        | $\sim 30$ [36]                       |
| <b>Polarimetric Differential Imaging (PDI)</b> | $1 \lambda/D$            | $\sim 30$ [38]                       |
| <b>Coherence Differential Imaging (CDI)</b>    | $1 \lambda/D$            | tbd                                  |

### 3. CURRENT XAO HIGH-CONTRAST INSTRUMENTS

The challenges and rewards of high contrast imaging have led to a massive effort in the development of extreme AO systems. The 672 actuator system at the LBT [39] could be considered a forerunner to extreme AO. A very similar system is currently in commissioning at the 6.5-m Magellan Telescope [40]. Both systems incorporate a PYRWFS and offer excellent correction performance down to visible wavelengths. The instrumentation and speckle calibration concept are however not specifically tuned to the high-contrast imaging case, but to a wider range of science cases.

The first truly high order system, with more than 3000 actuators on the DM, is P3K for the 5-m telescope at Palomar Observatory, which had its first light in June 2011 [41]. P3K is a very innovative system that is also used to test a number of novel concepts and technologies besides its regular observing program. This also holds for the SCEXAO system for the Subaru telescope [42], which is a second stage XAO system mounted behind the regular AO188 and incorporates a number of innovations such as a PIAA coronagraph with coronagraphic LOWFS, FPYRWFS and a MEMS DM.

Two dedicated X AO instruments will be SPHERE [43] and GPI [44], which are close to commissioning at the VLT and Gemini observatories. Both rely mostly on well-established technology such as the spatially-filtered SHWFS and come with massive amounts of observing time for the teams in order to conduct large surveys for comprehensive studies in Exoplanet science.

Table 2 lists Current XAO high-contrast imagers and some of their characteristics.

**Table 2.** Current XAO high-contrast imagers and some of their characteristics.

|               | <b>DM</b>                     | <b>WFS</b>                 | <b>Features</b>                        | <b>Speed</b>                        | <b>Res. WFE</b>                 | <b>Speckle Calib</b> | <b>Status</b>                         |
|---------------|-------------------------------|----------------------------|--|-------------------------------------|---------------------------------|----------------------|---------------------------------------|
| <b>FLAO</b>   | DSM,<br>672 Act               | PYRWFS<br>3 / 6 I/D<br>mod | -                                      | ~30 Hz, 0<br>dB, 900 Hz<br>framrate | ~120 nm<br>rms<br>(sky)         | ADI                  | In operation                          |
| <b>MagAO</b>  | DSM,<br>585 Act               | PYRWFS                     | Vibr. Ctrl,<br>Vis Cam                 | 1 kHz<br>framerate                  | ~100-<br>120 nm<br>rms<br>(lab) | SDI, ADI             | Installation at<br>telescope          |
| <b>P3K</b>    | Piezo,<br>241+3388<br>Act     | SF-SHS,<br>quad-cell       | Woofers/<br>Tweeter.<br>CALSYS,<br>VVC | ~70 Hz, 0<br>db, 2 kHz<br>framerate | ~150 nm<br>rms<br>(sky)         | SD,<br>SDI           | In operation                          |
| <b>SCEXAO</b> | Bimorph 188<br>+ MEMS 1k      | PYRWFS<br>no mod           | CLOWFS<br>PIAA,<br>Vis Cam             | 1 kHz                               | Tbd                             | SDI,<br>ADI          | Partly in<br>operation,<br>upgr. path |
| <b>GPI</b>    | Piezo ~100 +<br>~1500<br>MEMS | SF-SHS,<br>quad-cell       | Woofers/<br>Tweeter.<br>CALSYS         | 1.2 kHz<br>framerate                | 24 nm<br>in-band                | SDI,<br>ADI, PDI     | 1 <sup>st</sup> light<br>Spring '13   |
| <b>SPHERE</b> | Piezo<br>1377 Act             | SF-SHS,<br>6px subap       | Vibr. Ctrl,<br>Vis Cam                 | ~ 100 Hz, 0<br>dB, 1.2 kHz<br>frame | ~100 nm<br>rms<br>(lab)         | SD, SDI,<br>PDI, ADI | 1 <sup>st</sup> light<br>Spring '13   |

#### 4. CONCLUSIONS

XAO high-contrast imaging is one important aspect of Exoplanet research, the future leading Science Case in Astronomy and for extremely large telescopes in particular. The science requires us to push for small inner working angles of tens of milliarcseconds, close to the near-infrared diffraction limit of even the largest telescopes. Several such instruments for 8-m class telescopes are already existing or about to take off, and the level of high-contrast imaging know-how has enormously increased over the past years. The success of these instruments will not only lead to extremely exciting science results, but will also be a major selling argument for the future extremely large telescopes.

With many thanks for very valuable contributions and comments to Jean-Luc Beuzit, Laird Close, Richard Dekany, Simone Esposito, Olivier Guyon, Bruce Macintosh & Cyril Petit.

#### REFERENCES

- [1] Cassan, A. et al., "One or more bound planets per Milky Way star from microlensing observations", Nature 481, Issue 7380 (2012)



- [2] Bonfils, X. et al., "The HARPS search for southern extra-solar planets XXXI. The M-dwarf sample", submitted to A&A (2012)
- [3] Marois, C. et al., "Images of a fourth planet orbiting HR 8799", Nature 468 (2010)
- [4] Lagrange, A. M. et al., "A Giant Planet Imaged in the Disk of the Young Star  $\beta$  Pictoris", Science 329 (2010)
- [5] Kaltenegger, L. and Traub, W., "Transits of Earth-like planets", ApJ 698 (2009)
- [6] Masciadri, E. et al., "A Search for Hot Massive Extrasolar Planets around Nearby Young Stars with the Adaptive Optics System NACO", ApJ 625 (2005)
- [7] Biller, B.A. et al., "An Imaging Survey for Extrasolar Planets around 45 Close, Young Stars with the Simultaneous Differential Imager at the Very Large Telescope and MMT", ApJS 173 (2007)
- [8] Lafreniere, D. et al., "The Gemini Deep Planet Survey", ApJ 670 (2007)
- [9] Kasper, M. et al., "A novel L-band imaging search for giant planets in the Tucana and  $\beta$  Pictoris moving groups", A&A 472 (2007)
- [10] Leconte, J. et al., "The Lyot Project Direct Imaging Survey of Substellar Companions: Statistical Analysis and Information from Nondetections", ApJ 716 (2010)
- [11] Janson, M et al., "High-contrast Imaging Search for Planets and Brown Dwarfs around the Most Massive Stars in the Solar Neighborhood", ApJ 736 (2011)
- [12] Delorme, P. et al., "High-resolution imaging of young M-type stars of the solar neighbourhood: probing for companions down to the mass of Jupiter", A&A 539 (2012)
- [13] Vigan, A. et al., "The International Deep Planet Survey I. The frequency of wide-orbit massive planets around A-stars", Accepted for publication in A&A
- [14] Bonavita, M. et al., "MESS (multi-purpose exoplanet simulation system)", A&A 537 (2012)
- [15] Kasper, M. et al., "EPICS: direct imaging of exoplanets with the E-ELT", Proc. SPIE 7735 (2010)
- [16] Guyon O., "Limits of Adaptive Optics for High-Contrast Imaging", ApJ 629 (2005)
- [17] Arcidiacono, C. et al., "An update of the on-sky performance of the layer-oriented wavefront sensor for MAD", Proc. SPIE 7736 (2010)
- [18] Clergeon, C.F. et al., "The Subaru coronagraphic extreme AO (SCEXAO) high sensitivity wavefront sensor: performance comparison between a non modulated pyramid and a non linear curvature wavefront sensor"
- [19] Ragazzoni, R., Farinato, J., "Sensitivity of a pyramidal Wave Front sensor in closed loop Adaptive Optics", A&A 350 (1999)
- [20] Poyneer, L. A., Véran, J.-P., "Toward feasible and effective predictive wavefront control for adaptive optics", Proc. SPIE 7015 (2008)
- [21] Devaney, N. et al., "Chromatic effects of the atmosphere on astronomical adaptive optics", ApOpt 47 (2008)
- [22] Guyon, O. et al., "Theoretical Limits on Extrasolar Terrestrial Planet Detection with Coronagraphs", ApJS 167 (2006)
- [23] Guyon, O. et al., "Coronagraphic Low-Order Wave-Front Sensor: Principle and Application to a Phase-Induced Amplitude Coronagraph", ApJ 693 (2009)
- [24] Petit, C. et al., "First laboratory validation of vibration filtering with LQG control law for Adaptive Optics", OptExpr 16 (2008)
- [25] Mawet D. et al., "Improved high-contrast imaging with on-axis telescopes using a multistage vortex coronagraph", Opt Letters 36 (2011)
- [26] Guyon, O. et al. "High Performance PIAA Coronagraphy with Complex Amplitude Focal Plane Masks", ApJS 190 (2010)
- [27] Give'on A. et al., "Broadband wavefront correction algorithm for high-contrast imaging systems", Proc. SPIE 6691 (2007)
- [28] Trauger, J. T., Traub, W. A., "A laboratory demonstration of the capability to image an Earth-like extrasolar planet", Nature 446 (2007)
- [29] Snik F. et al., "The Vector-APP: a Broadband Apodizing Phase Plate that yields Complementary PSFs", Proc. SPIE 8450 (2012)
- [30] Carlotti, A. et al., "Optimal pupil apodizations of arbitrary apertures for high-contrast imaging", OptExpr 19 (2011)
- [31] Crepp, J.R. et al., "Speckle Suppression with the Project 1640 Integral Field Spectrograph", ApJ 729 (2011)
- [32] Marois, C. et al., "Differential Imaging with a Multicolor Detector Assembly: A New Exoplanet Finder Concept", ApJ 615 (2004)
- [33] Sparks, W. B., Ford, H.C., "Imaging Spectroscopy for Extrasolar Planet Detection", ApJ 578 (2002)

- [34] Gladysz, S. et al., "Statistics of intensity in adaptive-optics images and their usefulness for detection and photometry of exoplanets", *JOSAA* 27 (2010)
- [35] Marois, C. et al., "Angular Differential Imaging: A Powerful High-Contrast Imaging Technique", *ApJ* 641 (2006)
- [36] Lafrenière, D. et al., "A New Algorithm for Point-Spread Function Subtraction in High-Contrast Imaging: A Demonstration with Angular Differential Imaging", *ApJ* 660 (2007)
- [37] Biller, B. et al., "An Imaging Survey for Extrasolar Planets around 45 Close, Young Stars with the Simultaneous Differential Imager at the Very Large Telescope and MMT", *ApJS* 173 (2007)
- [38] Perrin, M. et al., "The IRCAL Polarimeter: Design, Calibration, and Data Reduction for an Adaptive Optics Imaging Polarimeter", *PASP* 120 (2008)
- [39] Esposito, S. et al., "First light AO (FLAO) system for LBT: final integration, acceptance test in Europe, and preliminary on-sky commissioning results", *Proc. SPIE* 7736 (2010)
- [40] Close, L.M., et al., "The Magellan Telescope Adaptive Secondary AO System: a visible and mid-IR AO facility", *Proc. SPIE* 7736 (2010)
- [41] Dekany R. et al. in the 2nd international conference on Adaptive Optics for Extremely Large Telescopes (2011)
- [42] Martinache F., Guyon O., "The Subaru Coronagraphic Extreme-AO Project", *Proc. SPIE*, 7440 (2009)
- [43] Beuzit J.-L., et al., "SPHERE: A Planet Finder Instrument for the VLT", *The Messenger* 125 (2006)
- [44] Macintosh B. et al., "The Gemini Planet Imager: from science to design to construction", *Proc. SPIE* 7015 (2008)